Molecular Therapy
Methods & Clinical Development
Original Article

Efficacy of HSV-TK/GCV system suicide gene therapy using SHED expressing modified HSV-TK against lung cancer brain metastases

Tomoya Oishi,[1] Masahiko Ito,[2] Shinichiro Koizumi,[1] Makoto Horikawa,[1] Taisuke Yamamoto,[1] Satoru Yamagishi,[3,4] Tomohiro Yamasaki,[1] Tetsuro Sameshima,[1] Tetsuro Suzuki,[2] Haruhiko Sugimura,[5] Hiroki Namba,[6] and Kazuhiko Kurozumi[1]

[1]Department of Neurosurgery, Hamamatsu University School of Medicine, Hamamatsu, Japan; [2]Department of Virology and Parasitology, Hamamatsu University School of Medicine, Hamamatsu, Japan; [3]Department of Organ and Tissue Anatomy, Hamamatsu University School of Medicine, Hamamatsu, Japan; [4]Preeminent Medical Photonics Education and Research Center, Hamamatsu University School of Medicine, Hamamatsu, Japan; [5]Department of Tumor Pathology, Hamamatsu University School of Medicine, Hamamatsu, Japan; [6]Department of Neurosurgery, Enshu Hospital, Hamamatsu, Japan

Lung cancer is one of the most common cancers, and the number of patients with intracranial metastases is increasing. Previously, we developed an enzyme prodrug suicide gene therapy based on the herpes simplex virus thymidine kinase (HSV-TK)/ganciclovir (GCV) system using various mesenchymal stem cells to induce apoptosis in malignant gliomas through bystander killing effects. Here, we describe stem cells from human exfoliated deciduous teeth (SHED) as gene vehicles of the TK/GCV system against a brain metastasis model of non-small cell lung cancer (NSCLC). We introduced the A168H mutant TK (TK^{A168H}) into SHED to establish the therapeutic cells because of the latent toxicity of wild type. SHED expressing TK^{A168H} (SHED-TK) exhibited chemotaxis to the conditioned medium of NSCLC and migrated toward implanted NSCLC *in vivo*. SHED-TK demonstrated a strong bystander effect *in vitro* and *in vivo* and completely eradicated H1299 NSCLC in the brain. SHED-TK cells implanted intratumorally followed by GCV administration significantly suppressed the growth of H1299 and improved survival time. These results indicate that the TK^{A168H} variant is suitable for establishing therapeutic cells and that intratumoral injection of SHED-TK followed by GCV administration may be a useful strategy for therapeutic approaches.

INTRODUCTION

Lung cancer is the most common malignant tumor and the leading cause of death in cancer patients.[1] Brain metastasis is found in 20% of patients at diagnosis, and up to 80% of patients suffer from brain metastasis over the disease course. The median survival of patients with brain metastasis of non-small cell lung cancer (NSCLC) is estimated to be 3–15 months.[2,3] The development of local and systemic treatments, such as molecularly targeted drugs, immunotherapies, surgery, and radiotherapy, improved the control of primary and intracranial metastatic lesions and prolonged overall survival. However, approximately 10% of NSCLC patients with brain metastases die from lesions in the central nervous system,[4] and the neurological cause of death is expected to increase in the future.[5] Therefore, novel therapeutic strategies for metastatic brain tumors are required.

Suicide gene therapy was first reported in the 1990s.[6,7] The thymidine kinase (TK)/ganciclovir (GCV) system is a gene-directed enzyme prodrug therapy. The *herpes simplex virus 1 thymidine kinase (HSV-TK)* gene, called the suicide gene, introduced into cells phosphorylates a prodrug, GCV, to the monophosphate form in the introduced cells. After that, it is phosphorylated by intracellular TK to the triphosphorylated form, which inhibits DNA synthesis and causes cell apoptosis. In addition, phosphorylated GCV is passively transferred to surrounding HSV-TK-nonexpressing cells through gap junction intercellular communication and induces surrounding cell death. This is the so-called bystander effect and is important for enhancing the antitumor effect of the TK/GCV system.[8,9] Since the phosphorylated form of GCV inhibits DNA synthesis, suicide gene therapy is likely to be effective against cells with active DNA synthesis, such as tumor cells;[10] it is possible to kill the tumor cells superselectively. We introduced HSV-TK into several kinds of stem cells and reported the effectiveness of suicide gene therapy using stem cells as vehicles in previous reports.[8,9,11] It is advantageous to use stem cells as vehicles of the suicide gene to treat tumors because they have a strong migration ability to especially invasive tumors.

Mesenchymal stem cells (MSCs) have an excellent self-renewal ability and multipotency and are being actively studied mainly in regenerative medicine. Stem cells from human exfoliated deciduous teeth (SHED) and dental pulp stem cells (DPSCs) are stem cells that are

Received 7 April 2022; accepted 3 July 2022;
https://doi.org/10.1016/j.omtm.2022.07.001.

Correspondence: Kazuhiko Kurozumi, Department of Neurosurgery, Hamamatsu University School of Medicine, 1-20-1 Handayama, Higashi-ku, Hamamatsu City, Shizuoka 431-3192, Japan.
E-mail: kurozu20@hama-med.ac.jp

isolated from the dental pulp and originate from the cranial neural crest. They have properties similar to mesenchymal stem cells and have the ability to differentiate into various tissue cells.[12,13] SHED have a higher proliferative ability than other mesenchymal stem cells;[14,15] however, the migration ability of SHED toward the tumor has not been fully studied. In addition, especially with regard to exfoliated deciduous teeth, it is easily available for dental treatments noninvasively or less invasively, so ethical concerns are small and have attracted attention in the field of regenerative medicine in recent years.[16]

However, it has been recently reported that the transduction of TK into stem cells causes toxicity to stem cells due to the increased metabolism of thymidine, which TK inherently possesses.[17] This toxicity causes difficulties in the creation of therapeutic cells. We found that TK subtypes with mutations that promote GCV metabolism, which have already been discovered, are also effective in reducing TK toxicity to SHED and can effectively treat mouse models of lung cancer brain metastatic lesions.

RESULTS

Establishment of SHED expressing HSV-TK as treatment cells

Amplified HSVTK-internal ribosome entry site 2 (IRES2)-*Aequorea coerulescens* green fluorescent protein (AcGFP) was cloned into a lentiviral vector to prepare pCSII-EF1α-HSVTK-IRES2-AcGFP (TK^{wt}) (Figure 1A). Subsequently, pCSII-EF1α-HSVTK-IRES2-AcGFP with a mutation of A168H in HSVTK (TK^{A168H}) and pCSII-EF1α-AcGFP (GFP) were also created. First, we set up the best conditions for creating SHED expressing TK. Each lentivirus containing TK^{wt}, TK^{A168H}, and GFP as a control was infected with SHED at a multiplicity of infection (MOI) = 2, 4, 6, respectively. The transduction efficiency of each lentivirus measured by GFP fluorescence was significantly increased in GFP, TK^{wt}, and TK^{A168H} as the MOI increased from MOI = 2 to MOI = 4, and a gradual increase was observed in the infection conditions from MOI = 4 to MOI = 6 (Figure 1B). Representative histograms of GFP fluorescence and cell number for each sample obtained by flow cytometric analysis are presented in Figure S1. The expression levels of HSV-TK protein on day 3 after infection were quantified by western blotting. HSV-TK protein expression was increased in an MOI-dependent manner, with no significant difference for TK^{wt} and TK^{A168H} at the same MOIs (Figure 1C).

Second, we compared the effects of lentiviral transduction of GFP, TK^{wt}, and TK^{A168H} into SHED at each MOI on cell viability and toxicity. To establish SHED expressing TK as treatment cells, a sufficient expression level is needed to obtain efficient GCV metabolism, but direct toxicity against SHED should be avoided as much as possible. The viability on day 5 after transduction showed a significant decrease at all MOIs of TK^{wt} compared to GFP as a control. TK^{A168H} showed no significant difference in viability at MOI = 2 compared to GFP and a significant decrease in viability in an MOI-dependent manner, although viability was relatively preserved at MOI = 4 compared to TK^{wt} (Figure 1D, left). The viability of SHED expressing TK^{wt} continued to decrease until day 7 at all MOIs, while a viability decrease was observed only at MOI = 6 in SHED expressing TK^{A168H} (SHED-TK; see also Figure S2). To evaluate the toxicity of TK on SHED, we compared the activity of caspase 3/7 adjusted for the cell number at each MOI. Caspase 3/7 activity divided by cell viability was normalized to that on day 3. TK^{wt} and TK^{A168H} showed a significant increase in the activity of caspase 3/7 at MOIs = 4 and 6. However, the activation of caspase 3/7 at MOI = 4 was significantly suppressed in TK^{A168H} cells compared to TK^{wt} cells (Figure 1D, right). On day 7, TK^{wt} had significantly higher caspase 3/7 activity than GFP at all MOIs, and TK^{A168H} had significantly higher caspase 3/7 activity at only an MOI = 6. There was no difference in the activity of caspase 3/7 between TK^{A168H} and TK^{wt} at MOI = 6 (see also Figure S3). Therefore, based on the expression level of TK, transduction efficiency, viability, and apoptosis after transduction, the optimal condition for transducing TK into SHED is TK^{A168H} at an MOI = 4.

The transduction efficiency of TK^{A168H} with MOI = 4 was approximately 80.5% ± 1.5% (Figure 1B). The susceptibility of SHED-TK to GCV is shown in Figure 1E. A significant decrease in the number of cells was observed at a concentration of 0.3 μg/mL compared to SHED-naive cells, and most SHED-TK cells were susceptible at a GCV concentration of 3 μg/mL after 6 days of culture. The median lethal dose (LD_{50}) was 1.82 μg/mL. At high concentrations of GCV, cytotoxicity was also observed for SHED-naive cells, while there was almost no effect on SHED-naive cells at <30 μg/mL.

In vitro bystander effect

Next, we measured the antitumor effect of SHED-TK on NSCLC cell lines by the bystander tumor-killing effect under GCV *in vitro*. NSCLC cells (H1299, A549) at a cell number of 2×10^3 were cocultured with SHED-TK cells at various SHED-TK and tumor ratios. The viability under 3 μg/mL GCV was compared to that under 0 μg/mL GCV as a control (Figure 2A). Each of the tumor cell lines showed a significant decrease in the cell viability from 2,000:2,000 to 63:2,000. In particular, bystander tumor killing was observed in coculture with H1299 cells. No toxicity of GCV without SHED-TK to the tumor cells was observed in either cell line. To observe bystander tumor killing with time-lapse imaging, H1299 cells expressing red fluorescent protein (RFP) and SHED-TK were cocultured at a ratio of 1:1, and time-lapse images were taken from 24 to 72 h after adding 3 μg/mL GCV. Starting with this observation, suppression of cell division was observed in the presence of GCV. Cell death began after 24 h (48 h after adding GCV), and most tumor cells were killed after 72 h of observation (Figure 2B; Videos S1 and S2).

Matrigel invasion assay

A Matrigel invasion assay was performed to examine the migration ability of SHED-TK to tumors. The migration ability of SHED-TK toward each of the conditioned media of H1299 and A549 cells was evaluated.

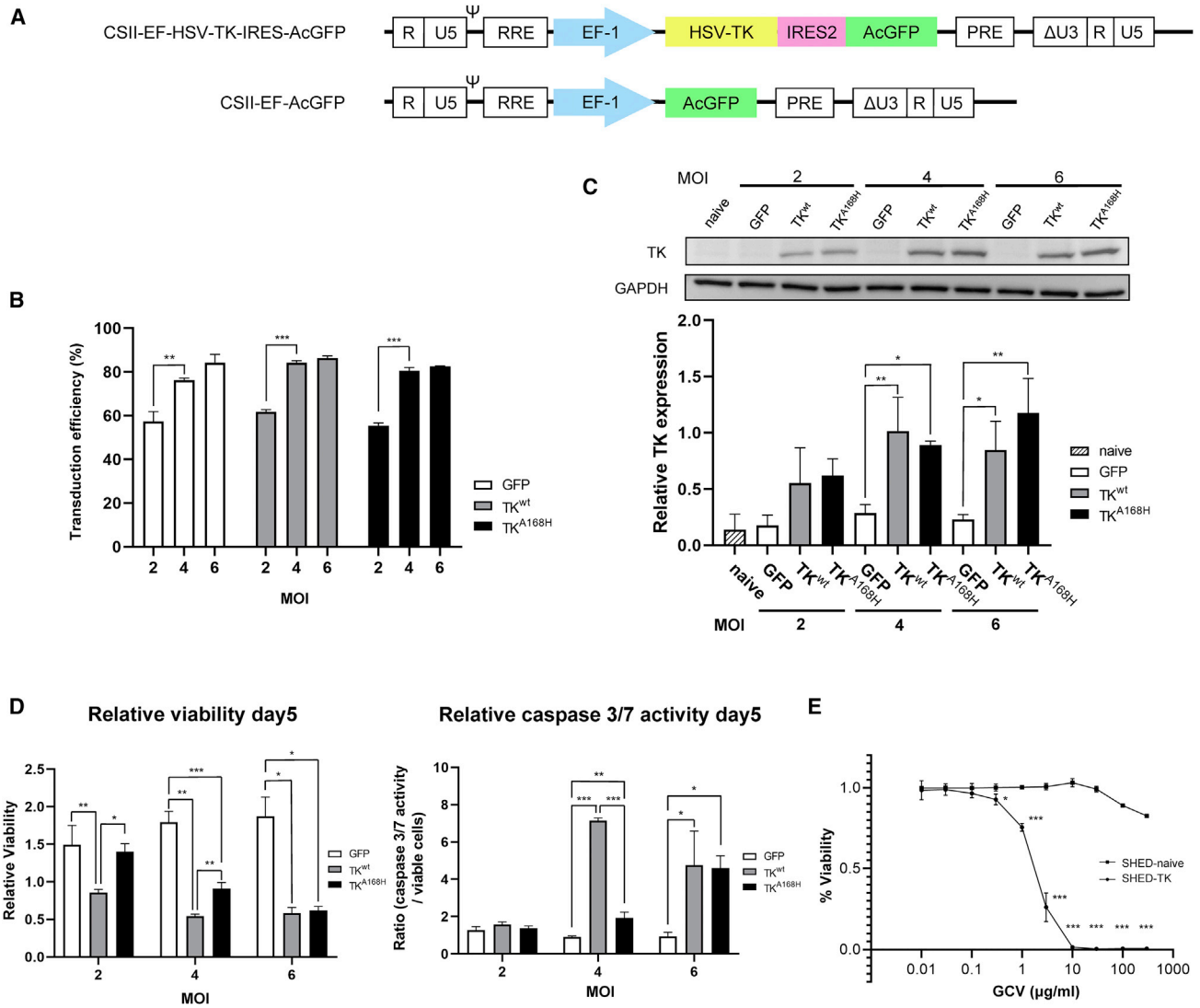

Figure 1. SHED-TK establishment and toxicity of TK to SHED

Schematic representation of the integrated proviral form of the lentiviral vector expressing the *HSV-TK* and *AcGFP* genes (A). The transduction efficiency of *TK* or *GFP* was increased in an MOI-dependent manner in TK ^{A168H}, TK^{wt}, and GFP cells, as analyzed by flow cytometry (n = 3; Tukey's test; means ± SDs; **p < 0.01; ***p < 0.001) (B). Western blot analysis of HSV-TK (40 kDa band) in SHED expressing TK^{wt}, TK^{A168H}, GFP, and SHED-naive (n = 3) shows an increase in TK expression in an MOI-dependent manner in TK^{wt} and TK^{A168H} cells. The results of TK protein expression are normalized to the internal control GAPDH (36 kDa band) and expressed as the mean ± SD (n = 3; Tukey's test; *p < 0.05; **p < 0.01). The y axis indicates the ratio of the quantified GAPDH band to that of the TK band (C). Cell viability and caspase 3/7 activity according to the viable cells on day 5 normalized to those of each sample of day 3 of SHED-transduced TK^{A168H}, TK^{wt}, and GFP (n = 4; Tukey's test; means ± SDs; *p < 0.05; **p < 0.01; ***p < 0.001) (D). There was a significant decrease in the relative viability of SHED transduced with TK^{wt} despite the low MOI. Viability is maintained in TK^{A168H} cells compared to TK^{wt} cells at MOIs = 2 and 4 (D, left). Caspase 3/7 activity in viable TK^{A168H} cells was significantly lower than that in TK^{wt} cells at an MOI = 4. The activity of caspase 3/7 in viable cells was significantly higher in TK^{wt} and TK^{A168H} cells infected at an MOI = 6 (D, right). GCV sensitivity of SHED-TK cells created by TK^{A168H} lentiviral infection at an MOI = 4. Significant cell death was observed at concentrations of 0.3 μg/mL or higher (n = 4; unpaired t test; means ± SDs;*p < 0.05; **p < 0.01; ***p < 0.001) (E).

Significant migration of SHED-TK cells to the conditioned medium of H1299 (Figure 3A) and A549 (Figure 3B) cells was observed.

In vivo bystander effect in the coimplantation tumor model

To observe the bystander effect *in vivo*, H1299 cells expressing luciferase (luc2) and RFP were coimplanted with SHED-TK into the right brain hemisphere of the nude mouse, and intraperitoneal GCV (50 mg/kg) twice per day (100 mg/kg/day) was administered on 10 consecutive days (H1299 + SHED-TK/GCV group) (Figure 4A). Three control groups were prepared: coimplantation with PBS administration (H1299 + SHED-TK/PBS group) and H1299 implantation with GCV or PBS administration (H1299 only/GCV group and

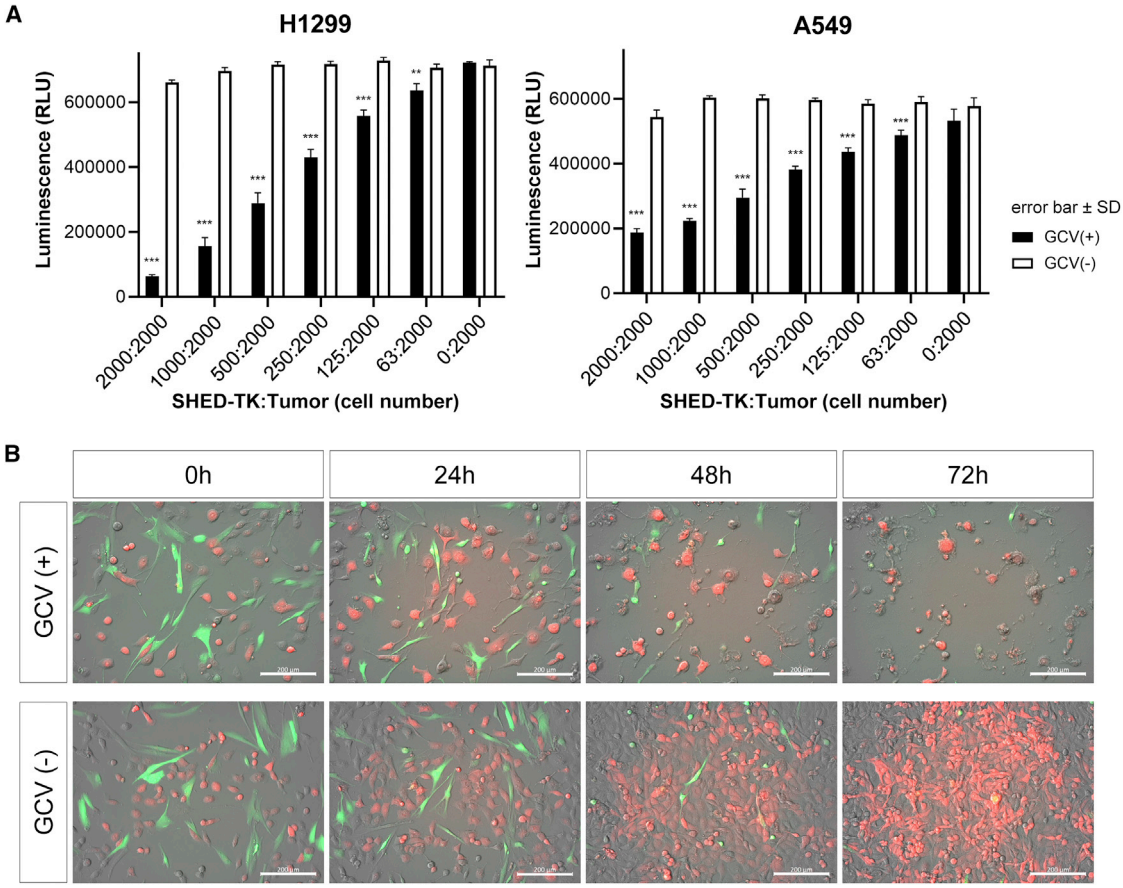

Figure 2. *In vitro* bystander effect between SHED-TK and NSCLC cells

Each graph shows the viability of H1299 and A549 cells cocultured with SHED-TK in medium containing 3 μg/mL GCV, GCV(+), or 0 μg/mL GCV, GCV(−) (n = 4; unpaired t test; means ± SDs; $^{**}p < 0.01$; $^{***}p < 0.001$). Tumor cell viability was significantly inhibited when the tumor cells and SHED-TK cells were exposed to GCV at a SHED-TK:tumor ratio as low as 63:2,000 (n = 4, means ± SDs; unpaired t test; $^{*}p < 0.05$; $^{**}p < 0.01$; $^{***}p < 0.001$) (A). Time-lapse images of the bystander effect between SHED-TK (green) and H1299 cells (red) observed under a culture microscope are shown (error bar, 200 μm) (B).

H1299 only/PBS group). The bioluminescence was increased due to tumor growth among the three control groups; however, a bioluminescence decrease due to tumor cell disappearance was observed in the H1299 + SHED-TK/GCV group (Figures 4B and 4C). A significant difference in bioluminescence was observed at 15 days after implantation.

Regarding survival time, no death was observed during the observation period in the H1299 + SHED-TK/GCV group, but the median survival times of each control group were 43 days for H1299 + SHED-TK/PBS, 47.5 days for H1299 only/GCV, and 41.5 days for H1299 only/PBS, and a significant prolongation of survival time was observed in H1299 + SHED-TK/GCV ($p < 0.001$) (Figure 4D). No obvious tumor formation was observed in the resected brain specimen of the H1299 + SHED-TK/GCV group, while prominent tumor formation was observed in each control group (Figure 4E). In the H1299 + SHED-TK/GCV group, tumor cells disappeared due to a strong bystander effect.

Tumor suppression effect of intratumoral implantation of SHED-TK

Since a significant antitumor effect was observed in the coimplantation model, the therapeutic effect on the brain metastasis tumor model was evaluated. As the treatment group, SHED-TK was implanted intratumorally on the fifth day after tumor implantation, and intraperitoneal GCV (50 mg/kg) twice per day (100 mg/kg/day) was administered for 10 consecutive days to examine the therapeutic effect of the TK/GCV system (SHED-TK/GCV group, n = 9) (Figure 5A). For the three control groups, SHED-TK was intratumorally implanted, PBS was intraperitoneally infused (SHED-TK/PBS group), and PBS was injected into the tumor, which was divided into a group to which GCV (PBS/GCV group) or PBS (PBS/PBS group) was administered (n = 9, respectively). After GCV administration, some mice in the SHED-TK/GCV group exhibited the disappearance of biological luminescence due to tumor shrinkage on day 18. However, the three control groups showed a significant increase in luminescence with tumor growth. Luminescence due to

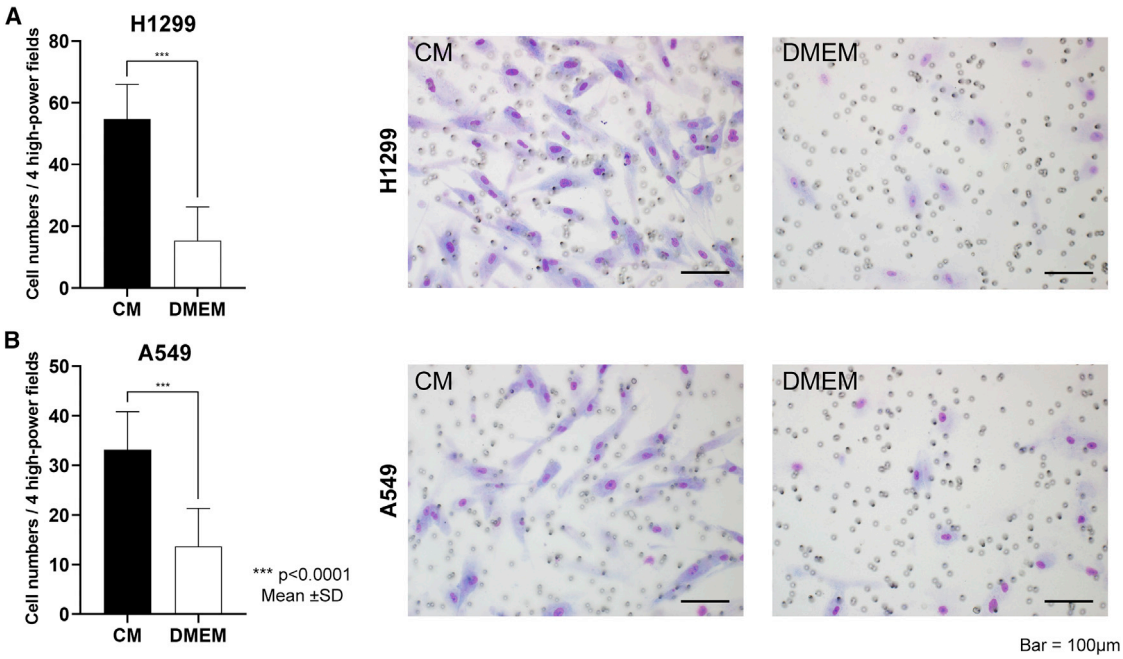

Figure 3. *In vitro* migration toward the conditioned medium of H1299 and A549 cells

The *in vitro* migratory capacity of SHED-TK cells toward NSCLC cells using a Matrigel invasion assay with conditioned medium of H1299 (A) and A549 (B) cells in the lower chamber (n = 3; means ± SDs; unpaired t test; ***p < 0.0001). Migrated SHED are stained by Diff-Quick staining, showing significant migration ability of SHED toward the conditioned medium.

tumor regrowth was observed in only one case by luminescence measurement on day 32 (Figures 5B and 5C). Additional luminescence measurements in the SHED-TK/GCV group performed on day 46 showed a significant increase in luminescence compared to that of day 32, even in the treatment group.

The Kaplan-Meier curve exhibited a significant prolongation of survival in the SHED-TK/GCV group compared to the three control groups. The median survival time of the SHED-TK/GCV group was prolonged to 135 days compared to that of each control group: 50 days in the SHED-TK/PBS group, 49 days in the PBS/GCV group, and 43 days in the PBS/PBS group (Figure 5D). Nevertheless, 5 mice in the SHED-TK/GCV group died of tumor growth before day 150, and 2 of 4 mice that survived 150 days in the SHED-TK/GCV group did not show any tumor formation (Figure 5E).

In vivo migration of contralateral implantation of SHED-TK

To evaluate the migration of SHED-TK toward the tumor mass in the mouse brain, H1299 cells expressing RFP were stereotactically implanted in the brain hemisphere, and SHED-TK cells were implanted 21 days after H1299 implantation in the hemisphere contralateral to that in which the tumor cells were implanted. Seven days later, the brain was extracted. Fluorescence microscopy images showed SHED-TK-labeled GFP migration into the tumor from the implantation site of the contralateral hemisphere (Figure 6). The large image of H1299 + SHED-TK (Figure 6) showed the tumor-implanted area (left hemisphere) and the SHED-implanted area (right hemisphere). In the representative magnified images of A and B, the white square in the large image, GFP + DAPI (upper row), and RFP + GFP (lower row), SHED emitting GFP fluorescence could be observed in the tumor. In the brain implanted with H1299 only, GFP fluorescence was not observed (Figure 6B).

DISCUSSION

The HSV-TK/GCV system using SHED as the suicide gene vehicle could be a treatment option for NSCLC brain metastases. SHED-TK cells have a prominent bystander effect on NSCLC cell lines, especially on H1299. SHED-TK has a significant migration ability to NSCLC. We substantiate the great efficacy of the combination of SHED-TK and GCV in the coimplantation model and preexisting tumor model. This suggests that SHED-TK had a sufficient antitumor effect due to its migration ability and bystander effect on tumors.

The ideal therapeutic cell for stem cell-based TK/GCV therapy is to maintain viability after TK transduction and to be able to metabolize GCV efficiently under GCV administration. It has been shown that the introduction of TK enhances thymidine (dT) metabolism, which is an intrinsic function of TK, resulting in the accumulation of thymidine triphosphate (dTTP) and cytotoxicity.[17] Therefore, ideal TK is considered to be less likely to metabolize dT and more likely to metabolize GCV. Previous biochemical experiments on TK variants have shown that the metabolism of dT and GCV differs depending on the TK mutation variant. Among the TK variants, A168H-mutated HSV-TK showed fully preserved GCV catalytic substrate activity

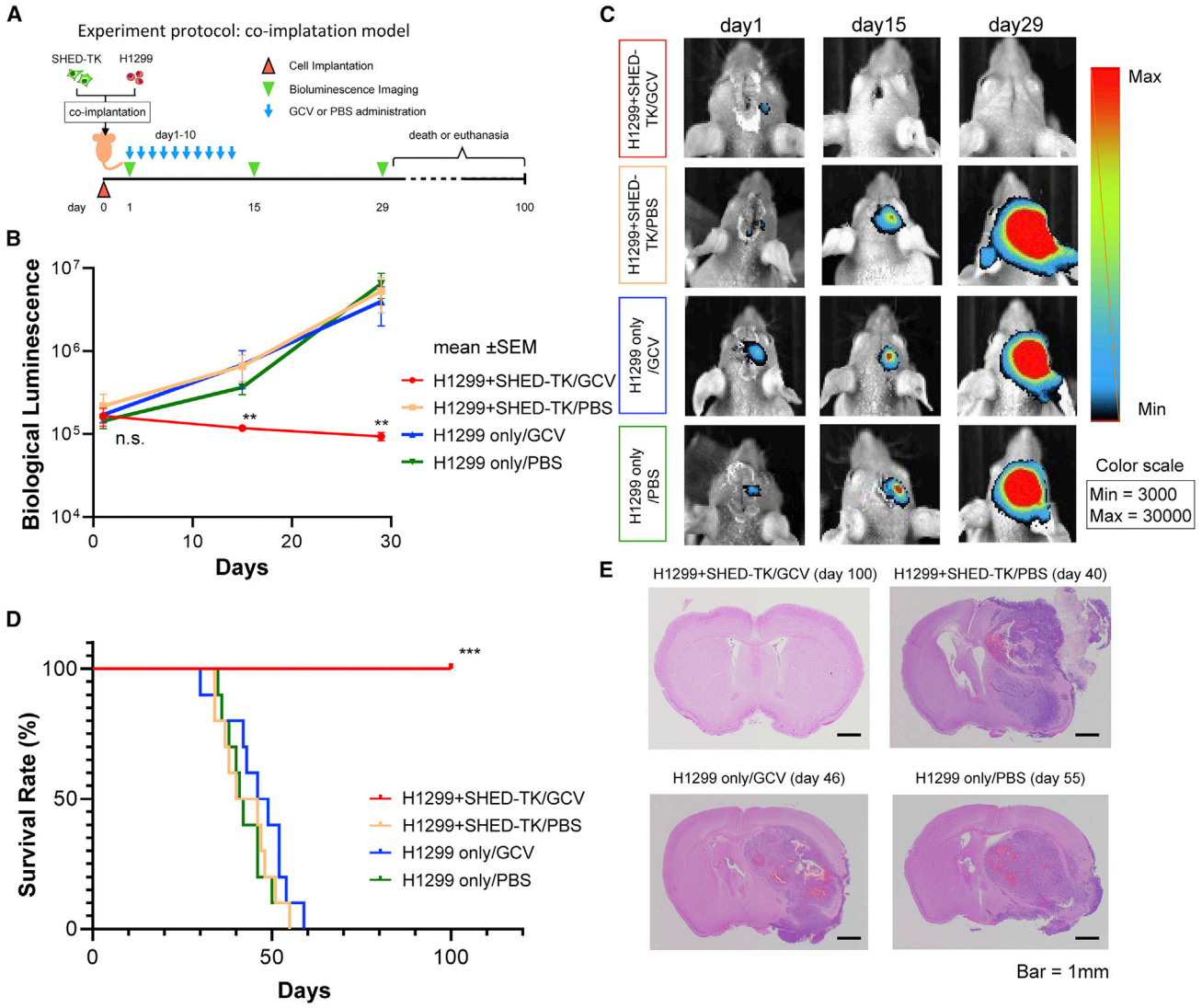

Figure 4. *In vivo* bystander effect between SHED-TK and H1299 in the brain

Experimental protocol of the *in vivo* bystander effect (A). The biological luminescence of each group at days 1, 15, and 29 (n = 10 each group, means ± SEMs; Dunn's test; **p < 0.01; n.s., not significant). The increase in the bioluminescent signal indicated tumor growth in the 3 control groups; however, the bioluminescent signal of the coimplantation and GCV-treated groups was decreased (B). Representative luminescent image of each group. The luminescent signal of the tumor vanished on day 15 (C). Survival time was also examined in the same mice used for the bioluminescent imaging experiment (n = 10 each group; log rank test; ***p < 0.001). No mice were dead in the coimplantation and GCV administration groups (D). Representative brain slices of each group are shown. Tumor formation was not observed in the coimplantation and GCV administration groups (E).

and heavily compromised dT kinase activity at the same time.[18] Although TK subtypes, transduction methods, stem cells, and GCV exposure times vary considerably among studies, GCV concentrations leading to 20% viability of GCV-exposed therapeutic cells range from 0.3 to 25 μg/mL.[8,9,19,20] Similar susceptibility was obtained in the present study at 3 μg/mL, suggesting that the GCV susceptibility of the treated cells is comparable to previous studies.

HSV-TK with this amino acid substitution has excellent therapeutic effects.[21,22] Preuss et al. reported that mutated HSV-TK (TK.007) with A168H amino acid substitution has high expression levels and excellent long duration bystander effects compared to wild-type TK in the introduction of HSV-TK into tumor cells.[21] Black et al. reported that SR39, another HSV-TK variant, possesses a lower IC_{50} of GCV and a higher tumor-suppressing effect than wild-type TK when used to transfect rat C6 glioma cells.[23] Balzarini et al. suggested that catalytic activity and affinity of the mutant enzymes could be affected by amino acids at positions 167 and 168, explained by structural context.[18] Hydrophobic and bulky side chains, such as phenylalanine, are the best residues to select for GCV activity. The mutations

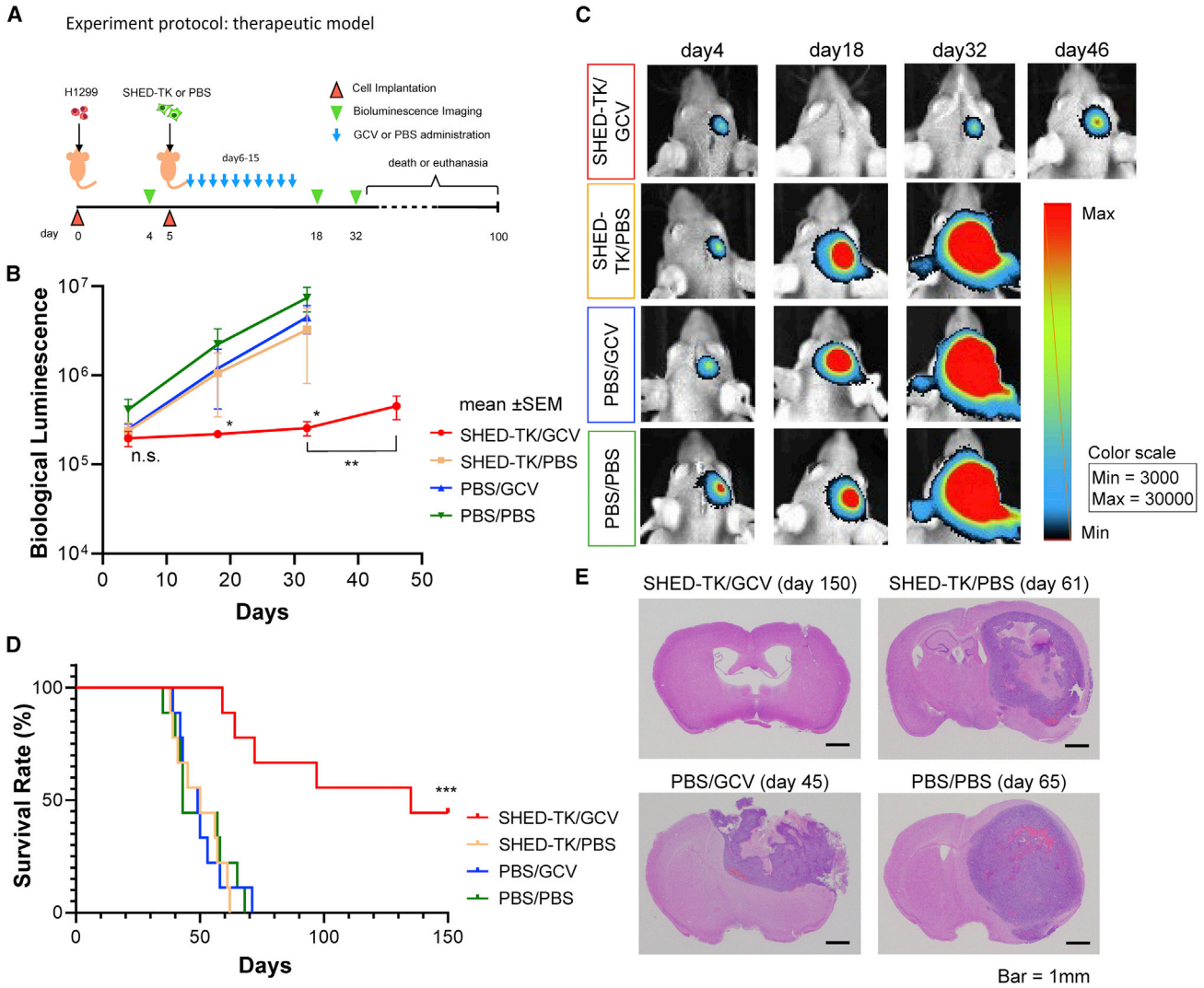

Figure 5. The inhibition of H1299 tumor growth in the brain by intratumoral injection of SHED-TK cells followed by GCV administration

Experimental protocol of tumor growth inhibition by intratumoral injection of SHED-TK (A). The biological luminescence of each group on days 4, 18, and 32 (n = 9 each group, means ± SEMs; Dunn's test; *p < 0.05; **p < 0.01; n.s., not significant). The significant increase in the bioluminescent signal of tumor growth in the 3 control groups was higher than that in the SHED-TK/GCV group (B). Representative luminescent image of each group (C). Survival time was examined in the same mice used for the bioluminescent imaging experiment (n = 9 each group; log rank test; ***p < 0.001). All H1299-bearing mice in the SHED-TK/PBS, PBS/GCV, and PBS/PBS groups died of the median tumor growth after 43–50 days, whereas the survival of the SHED-TK/GCV group was significantly longer than that of the other 3 groups (D). Representative brain slices of each group are shown (E).

at residue 168 have a lower discriminating power compared to residue 167; however, modification of residue 168 is located around dT, not GCV, and Lys and His residues are thought to inhibit dT, not GCV.[18] In the present study, TK^{A168H} was expected to contribute to the reduction of toxicity mainly by inhibiting the metabolism of dT. Although there has been only one study of TK^{A168H} transfection of stem cells,[24] the toxicity of TK to stem cells has not been well investigated. This is the first report showing that the A168H mutation suppresses TK-induced apoptosis in TK-introduced cells. We suppose that the optimization of HSV-TK with A168H is effective not only in improving GCV metabolic efficiency but also in reducing toxicity during TK transduction into stem cells.

In regard to the cause of the toxicity associated with the introduction of wild-type TK, Iwasawa et al. reported that excessive dT metabolism, which results in an imbalance of the nucleic acid pool, causes the cell-cycle blockade of stem cells.[17] The excessive dT metabolism caused by TK^{wt} is why TK^{wt} induces toxicity in SHED. We believe that TK-induced apoptosis can be suppressed by transducing TK^{A168H}, which has a low affinity for dT, although we did not

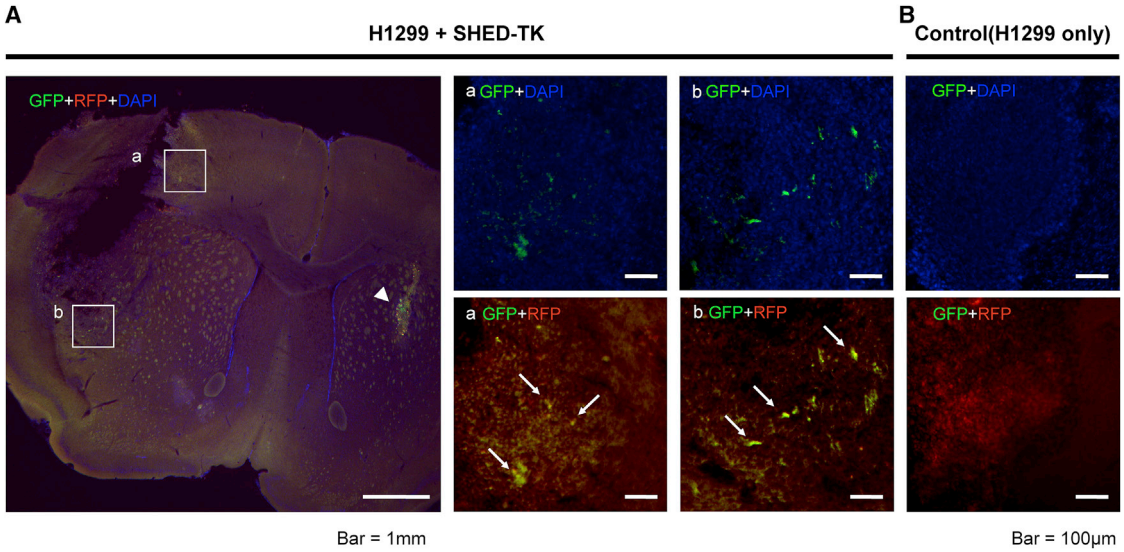

Figure 6. *In vivo* migration capacity of SHED-TK toward H1299 in the brain

SHED-TK cells implanted in the left hemisphere migrated toward the tumor mass of H1299 cells. SHED-TK was implanted into the striatum of the left hemisphere (arrowhead). SHED-TK (green) migration toward the tumor mass (red) was observed in the high-magnification images (a and b) (A). A GFP signal was not observed in the control brain without SHED-TK implantation (B).

measure the metabolic activity on dT and GCV with TK^{A168H} and TK^{wt}. Regarding the other method of reducing HSV-TK toxicity in stem cells, Tamura et al. reported the effectiveness of the Tet-inducible system to avoid constant expression of TK for transducing HSV-TK into induced pluripotent stem (iPS) cells to reduce its toxicity.[20] TK with the A168H mutation is considered an effective strategy to reduce toxicity to stem cells.

Our results suggest that the SHED-optimized TK/GCV system could be expected to have a sufficient therapeutic effect on suicide gene therapy for metastatic brain tumors. The effectiveness of suicide gene therapy using stem cells against various cancers, such as NSCLC, breast cancer, colon cancer, pancreatic cancer, and malignant melanoma, has been reported.[25–28] However, there are a few reports of suicide gene therapy using stem cells for brain metastasis.[29–31] Most of these reports are those using the cytosine deaminase (CD)/5-fluorocytosine (5-FC) system, and few use HSV-TK. Joo et al. reported the efficacy of CD-introduced neural stem cells on breast cancer brain metastasis.[29] Wang et al. reported a blood metastasis model and the antitumor effect of neural stem cells that express both CD and TK.[30] However, it has been reported that there are differences in the degree of activation of 5-FC or GCV depending on the type of tumor cells.[32] Although typical human NSCLC cell lines are used in this study, it has been reported that the susceptibility to the HSV-TK/GCV system is different among the cell lines; adenocarcinoma and large-cell lung cancer are relatively sensitive to GCV.[26] Another advantage of the TK/GCV system using stem cells is that it only attacks tumor cells in contact with stem cells because metabolized GCV can spread to neighboring cells only through gap junctions. Therefore, the advantage of the TK/GCV system is that it is less harmful to normal tissues.[10] In this study, a significant bystander tumor killing effect was observed against adenocarcinoma and large-cell lung carcinoma. Phase I and II clinical trials were performed for suicide gene therapy, especially for primary lesions of pancreatic cancer, prostate cancer, melanoma, hepatocellular carcinoma, and ovarian cancer.[33–36] However, for brain metastasis, suicide gene therapy is still in the animal experimental stage. Further research is required for clinical trials.

The advantage of using stem cells as vehicles for suicide genes is the high ability to migrate into tumors. In the glioma model, it has also been reported that neural stem cells and iPS cells accumulate in the hypoxic region in the brain and in tumor cell-related substances, stromal cell-derived factor-1, vascular endothelial growth factor (VEGF), and urokinase-type plasminogen activator.[37,38] SHED also have the ability to migrate to tumors and can be expected to have a therapeutic effect on highly invasive tumor cells that cannot be completely removed by surgery in clinical situations. Therapeutic cells migrate through neural tissues, and SHED with high neurotropism may efficiently migrate to the tumor. Moreover, damaged neural tissues by invading tumor cells may also attract therapeutic cells because SHED are known to have potent neurotropism.[16,39] DPSCs have been reported to have increased proliferative ability, migratory ability, and stem cell lineage markers (CXCR4, G-CSFR) under hypoxic conditions.[40] Therefore, it is possible that the tumor-induced hypoxic environment enhanced the migration ability of SHED to the metastatic lesion and enhanced the antitumor effect. The transfer of GCV metabolites through the gap junction between stem cells and tumor cells is also important.[41]

The ease of cell handling and ethical aspects for the selection of stem cells are crucial for cell therapy. SHED has several advantages. SHED can be obtained from deciduous teeth with minimal invasiveness, and

there are no major ethical issues to overcome. Moreover, SHED have many advantages over other types of MSCs, such as high proliferative potential, neuronal differentiation, and neurotrophic capacity.[42] The comparison of the speed of proliferation of SHED compared to DPSC is inconclusive.[43,44] It has been reported that SHED did not show spontaneous differentiation or degeneration in long-term culture.[44] SHED have higher proliferation ability and differentiation capacity than DPSC.[43] Although it has been pointed out that iPS cells may have malignant transformation,[45] no tumorigenesis has been reported at this time in SHED. As with other mesenchymal stem cells, early senescence, DNA damage during expansion, poor engraftment, and short-term survival after transplantation are major concerns for the clinical use of dental pulp stem cells, and introducing the human telomerase reverse transcriptase (hTERT) gene has been attempted to overcome these problems.[46]

NSCLC with epidermal growth factor receptor (EGFR) mutation or anaplastic lymphoma kinase (ALK) fusion gene is prone to intracranial metastasis, and intracranial metastasis occurs in 50%–60% of the disease course of NSCLC.[47] However, H1299 does not have such a driver mutation. Furthermore, it is necessary to examine whether this therapy is effective against cell lines with driver mutations. Metastatic brain tumors often occur in multiple locations in the brain. Another limitation of this study is that the mouse model in this experiment was created by directly implanting the tumor into the brain rather than using a fully metastatic brain tumor model resulting from hematogenous metastasis, and the single lesion was treated. It has been reported that extracellular vesicles (EVs) and exosomes secreted from stem cells are expected to be used as biological delivery vehicles for therapeutic agents.[48,49] EVs and exosomes can cross the blood-brain barrier and do not cause acute immune response and risk of tumor formation; thus, suicide gene therapy using EVs and exosomes could be a future therapeutic strategy for intracranial tumors.[50]

In conclusion, we showed that using TK^{A168H}, which metabolizes GCV more specifically, reduced the inherent toxic effect of TK on SHED, and SHED-TK followed by GCV administration suppressed tumor growth in an NSCLC brain metastasis model. We determined the optimal conditions for the lentiviral transduction of TK into SHED. These data show promising prospects for future clinical applications of stem cell-based gene therapy for brain metastases by using optimized TK to enhance its efficacy.

MATERIALS AND METHODS

Cell lines

Stem cells from human exfoliated deciduous teeth (SHED) were obtained from Kidswell BioScience (Tokyo, Japan) through a Material Transfer Agreement. SHED cells were cultured in 100 mm dishes with modified Eagle's medium-alpha (α-MEM) containing 10% fetal bovine serum (FBS) and 1% penicillin/streptomycin. The SHED cells were dissociated at 37°C for 5 min using TrypLE Select (Thermo Fisher Scientific, Waltham, MA). The passage number of SHED used in all of the experiments was 5–10. A549 and H1299, human NSCLC cell lines obtained from the American Type Culture Collection (ATCC), were cultured in 100 mm dishes with RPMI 1640 with 10% FBS. These cell lines were dissociated at 37°C for 5 min using Accutase solution (Sigma-Aldrich, St. Louis, MO) and passaged. For lentivirus production, 293T cells obtained from the RIKEN BioResource Research Center were cultured in type I collagen-coated 100 mm dishes with Dulbecco's modified Eagle's medium (DMEM) containing 10% FBS, 1% nonessential amino acids (Thermo Fisher Scientific), and 1% penicillin/streptomycin. These cells were dissociated with TrypLE Select. All of the cultures were incubated at 37°C with 5% CO_2.

Plasmid construction

HSV-TK-IRES2-AcGFP[9] in pWPXL-HSV-TK-IRES2-AcGFP was amplified by PCR. The amplified DNA fragment was cloned into the lentiviral vector pCSII-EF1α using InFusion HD (Takara Bio, Shiga, Japan). The amino acid sequence of *HSV-TK* (GenBank: J02224.1) reported by Wagner M (wild-type TK) was used in all of the experiments, and we described it as TK^{wt}.[51] Point mutations in *HSV-TK* were introduced by using KOD One PCR Master Mix (Toyobo, Osaka, Japan) and a pair of primers according to the manufacturer's protocol. For A168H amino acid substitution in *HSV-TK* (TK^{A168H}), the following primers were used: 5′-CGCCATCCCATC GCCCACCTCCTGTGCTACCCG-3′ and the reverse primer having its complimentary sequence. The final vector sequences were verified by DNA sequencing.

To establish tumor cells with stable expression of fluorescent protein and luciferase, the amplified *Luc2* was cloned into the multiple cloning site (MCS) of pFC-EF1-MCS-PGK-RFP-Puro using InFusion HD (Takara Bio).

Lentivirus preparation

Third-generation lentiviral packaging mixes, either pCSII-EF1α-$HSVTK^{wt}$-IRES2-AcGFP (TK^{wt}) or pCSII-EF1α-$HSVTK^{A168H}$-IRES2-AcGFP (TK^{A168H}) and pCSII-EF1α-AcGFP (GFP), were co-transfected into 293T cells by using Lipofectamine LTX Reagent and PLUS Reagent (Thermo Fisher Scientific) according to the manufacturer's instructions. Twelve hours after transfection, the cells were washed with fresh medium two times and cultured in medium containing viral boost reagent (Alstem, Richmond, CA) mixed with the medium following a fresh wash. The culture supernatant containing lentivirus was harvested at 36 and 72 h after transfection. Following filtration with a Sterivex-HV 0.45 μm pore polyvinylidene fluoride (PVDF) filter (Merck, Darmstadt, Germany), the supernatant was concentrated with Lentivirus Precipitation Solution #VC100 (Alstem). The pellet was diluted with DMEM with 10% FBS and stored at −75°C. To determine the viral titer of the lentiviral solution, SHED cells were infected with 10-fold diluted lentiviral supernatant. At 48 h after the infection, as mentioned below, the number of GFP^+ cells was counted by an InCell Analyzer 2200 (GE Healthcare, Chicago, IL). The titer was calculated by the number of GFP^+ cells in the well divided by the volume of viral solution in the well (focus forming unit [FFU]/mL).

Lentiviral infection

SHED passage 5 cells (2.4×10^5) were seeded in 6-well plates. The next day, the number of SHED cells in a well was counted, and the number of virus particles equal to the number of cells in the well was defined as MOI = 1. Lentivirus solution was diluted with fresh medium to MOIs of 2, 4, and 6 according to the experiment, and polybrene (Nacalai Tesque, Kyoto, Japan) was added to a final concentration of 8 μg/mL. The cells were washed with fresh medium 3 times and passaged at 24 and 48 h after lentiviral infection. At 3 days post-infection, HSV-TK expressing SHED was used in the following experiments.

Western blot

To assess the expression of HSV-1 TK in SHED cells infected with TK lentivirus, western blotting was conducted. SHED cells infected with TK lentivirus at MOIs of 2, 4, and 6 and naive SHED lentivirus as a control were seeded in 12-well plates. On day 3 of lentiviral infection, samples were treated with RIPA buffer containing the protease inhibitor cOmplete (Roche Diagnostics, Mannheim, Germany) and phosphatase inhibitor phosSTOP (Sigma-Aldrich). The lysates were collected, and the concentration of protein was measured by a Pierce BCA Protein Assay Kit (Thermo Fisher Scientific) and resuspended in Laemmli buffer at a concentration of 10 μg/15 μL followed by 3 min of boiling at 95°C. A total of 10 μg protein was loaded into each lane of a TGX gel (BioRad Laboratories, Hercules, CA). Sodium dodecyl sulfate-polyacrylamide gel electrophoresis (SDS-PAGE) was conducted, and the obtained bands were transferred to PVDF membranes using a tank-type blotting apparatus. After blocking with Block ACE (KAC, Amagasaki, Japan), the membrane was subjected to anti-HSV-1 thymidine kinase antibody (vL-20 sc-28038) (Santa Cruz Biotechnology, Dallas, TX) (1:5,000). The control band was detected by anti-glyceraldehyde 3-phosphate dehydrogenase (GAPDH) antibody (6C5) (Santa Cruz Biotechnology) (1:5,000), followed by immersion with anti-goat immunoglobulin G (IgG) for anti-HSV-1 TK and anti-rabbit for anti-GAPDH, both of which were conjugated with horseradish peroxidase (HRP) (1:10,000). Protein bands were detected by a chemiluminescence imager (FUSION FX.7 EDGE, Vilber Lourmat, Collegien, France) after reaction by ECL substrate solution. The quantification of band intensities was performed using ImageJ (NIH, Bethesda, MD).

Flow cytometry

SHED were infected with lentivirus at MOIs of 2, 4, and 6, as described above. Cells were dissociated, and the percentage of cells with a relative fluorescence intensity of GFP greater than 10^1 relative to the gated total cell number was counted using flow cytometry (Gallios, Beckman Coulter, Brea, CA). The threshold of GFP fluorescence was set as the upper limit of GFP fluorescence of SHED-naive cells.

Viability and caspase 3/7 assay

Viability and caspase 3/7 activity were qualified using the ApoTox-Glo Triplex assay (Promega Corporation, Madison, WI). SHED-infected GFP, TK^{A168H}, and TK^{wt} lentiviruses at MOIs of 2, 4, and 6, respectively, were seeded in black clear-bottom 96-well plates at 5 10^3 cells/well. Viability and caspase 3/7 activity were qualified at days 3, 5, and 7 after lentiviral infection according to the manufacturer's protocol. Briefly, 24 h after seeding, each well was washed with fresh media. Then, the cells were incubated for 3, 5, or 7 days following infection, and the medium was changed every other day. Cells were incubated for 1.5 h with viability/toxicity reagent, and fluorescence was measured using a Synergy H1 96-well plate reader (BioTek Instruments, Winooski, VT). Then, the cells were incubated for 2 h at room temperature with Caspase-Glo reagent, and luminescence was measured using Synergy H1. The activity of caspase 3/7 per number of viable cells was calculated by dividing the value from the caspase-glo 3/7 assay by that from the cell viability. The relative cell viability and relative activity of caspase 3/7 per cell viability were calculated by the assay results on day 3 after lentiviral infection as 1 and the results on days 5 and 7 as a ratio to day 3.

Preparation of H1299 expressing RFP and Luciferase2

The pFC-EF1-MCS-PGK-RFP-Puro and PhiC-31 integrase expression vectors (System Biosciences, Palo Alto, CA) were cotransfected into H1299 cells seeded in 100-mm plates with Lipofectamine LTX. The cells were washed with fresh medium 12 h after transfection. The cells were cultured with 2 μg/mL puromycin (InvivoGen, San Diego, CA) for 7 days after transfection. Thereafter, the cells were passaged, and the RFP-expressing cells were sorted with the cell sorter MoFlo Astrios (Beckman Coulter).

GCV sensitivity of SHED-TK

SHED-TK or SHED-naive cells were seeded in a 96-well plate at a density of 5×10^3 cells per well. α-MEM containing 10% FBS and various concentrations (0.01–300 μg/mL) of GCV (Fujifilm Wako Pure Chemical Corporation, Osaka, Japan) and 0 μg GCV as a control were prepared, and the cells were incubated for 7 days. The number of living cells was determined by an ATP assay using CellTiter Glo (Promega Corporation) according to the manufacturer's protocol, and the percentage of viability was expressed as the percentage luminescence of each GCV concentration compared to the control (0 μg/mL).[9] The luminescence of each well was measured by Synergy H1.

In vitro bystander effect assay

A total of 2×10^3 NSCLC cell lines (H1299, A549) were seeded in each well of a 96-well plate. SHED-TK was added at various ratios (SHED-TK:tumor, 63–2,000:2,000), and control wells (each NSCLC cell line only) were prepared. GCV (3 μg/mL) was administered to the experimental group, and the medium was changed every other day. The number of living cells was determined by CellTiter Glo after 4 days of exposure to GCV.

Time-lapse imaging

The bystander effect was observed with a Celldiscoverer 7 (Carl Zeiss, Oberkochen, Germany). The same number of H1299 cells expressing RFP (H1299-RFP-luc2) and SHED-TK expressing AcGFP were co-cultured in 6-well plates. GCV (3 μg/mL) was administered the

next day. After additional replacement with 4 mL of fresh medium with 3 μg/mL GCV at 24 h after GCV administration, the plate was placed in Celldiscoverer 7 to collect time-lapse images for 72 h. The frames were taken in 20-min intervals.

Animals and surgical procedures

Experiments were conducted in accordance with the guidelines approved by the Animal Care Committee at the Hamamatsu University School of Medicine Animal Care Facility (approved number: 2020092). Female BALB/c slc nu/nu mice (18–22 g, 7 weeks old, Nippon SLC, Hamamatsu, Japan) were anesthetized with a mixture of 0.75 mg/kg medetomidine (Nippon Zenyaku Kogyo, Koriyama, Japan), 4.0 mg/kg midazolam (Fuji Pharma, Tokyo, Japan), and 5.0 mg/kg butorphanol (Meiji Seika Pharma, Tokyo, Japan) by intraperitoneal injection. A sagittal incision was made on the midline of the head, and a burr hole was placed 2.5 mm lateral to bregma on the right brain. A 26-G needle was inserted at a depth of 3.5 mm from the brain surface with stereotactic guidance (Narishige, Tokyo, Japan), kept in position for 1 min, and then withdrawn to a depth of 3 mm. The cells were infused for 5 min. The needle was kept for 1 min and removed gradually over 3 min. After the operation, the mice were awakened from anesthesia by intraperitoneal injection of antisedan (Nippon Zenyaku Kogyo). The mouse was euthanized if the mouse had >20% weight loss, severe paresis, ataxia, or seizure in the observation period. The brains were resected and obtained for histologic examination.

In vivo bystander effect between SHED-TK and H1299-luc cells in the nude mouse intracranial tumor model

Forty female nude mice were anesthetized, and the tumor and SHED-TK (H1299 + SHED-TK) or tumor cells (H1299 only) were implanted as described above. In the coimplantation group, 5×10^4 H1299-RFP-luc2 cells mixed with the same number of SHED-TK cells in 5 μL RPMI 1640 were implanted into the right brain of nude mice. In the tumor implantation group, 5×10^4 H1299-RFP-luc2 cells in 5 μL RPMI 1640 were similarly implanted. The mice were intraperitoneally injected with GCV (50 mg/kg body weight in 200 μL PBS) or PBS twice per day from day 1 after tumor implantation for 10 consecutive days.[9]

Biological luminescence imaging of H1299-RFP-luc2 was performed by Fusion FX.7 EDGE (Vilber-Lourmat) on days 1, 15, and 29 after tumor implantation. The luminescence signals were measured by a charged-coupled device (CCD) camera in Fusion FX.7 10 min after the intraperitoneal injection of 150 mg/kg XenoLight Rediject D-luciferin (PerkinElmer, Waltham, MA). The exposure time was 2 min.

Intratumoral injection of SHED-TK cells followed by GCV administration

A total of 36 female BALB/c slc nu/nu mice were anesthetized, and 5×10^4 H1299-RFP-luc2 cells were stereotactically implanted, as previously mentioned. Five days after H1299 implantation, 5×10^4 SHED-TK cells were stereotactically implanted in the tumor site. The mice were intraperitoneally injected with GCV (50 mg/kg body weight in 200 μL PBS) or PBS twice per day from day 6 after tumor implantation for 10 consecutive days. Biological luminescence imaging of H1299-RFP-luc2 was performed under the aforementioned conditions on days 4, 18, 32, and 46 after tumor implantation.

In vivo migration of SHED-TK toward NSCLC cells

A total of 5×10^4 H1299 cells were implanted into the brain of a nude mouse as described above, and 21 days later, 5×10^5 SHED-TK cells were implanted into the opposite side. Seven days after SHED-TK implantation, the mouse was euthanized by the above method, fixed by perfusion with 4% paraformaldehyde (PFA), and the brain was carefully removed. Additional fixation was performed by immersion into 4% PFA at 4°C for 6 h and transferred to 30% sucrose in PBS, embedded in an optimum cutting temperature compound (OCT, Sakura Finetek Japan, Tokyo, Japan), sliced into 50-μm-thick sections with a cryostat, stained with Hoechst 33342 diluted 1:10,000, and mounted on glass slides.

Statistical analysis

The statistical significance of the difference was determined by an unpaired Student's t test for comparison between the two groups. For comparison of three or more groups, one-way ANOVA was performed when the variances were equal, and Tukey's test was used for post hoc analyses. If the variances were not equal, then the Kruskal-Wallis test was performed, and Dunn's multiple comparisons test was used for post hoc comparisons. The survival data were log rank tested based on the Kaplan-Meier curve. The significance level was $p < 0.05$ in all of the tests. All of the data were analyzed with GraphPad Prism 8 (GraphPad Software, San Diego, CA).

Data availability

The authors declare that all of the data supporting the findings of this study are available within the article and its supplemental information files. Raw data can be provided upon reasonable request.

SUPPLEMENTAL INFORMATION

Supplemental information can be found online at https://doi.org/10.1016/j.omtm.2022.07.001.

ACKNOWLEDGMENTS

We thank all of the members in the laboratory and Yasuyuki Mitani (Kidswell BioScience, Tokyo, Japan) for discussions and suggestions. Part of this work was performed at the Advanced Research Facilities & Services (ARFS), Hamamatsu University School of Medicine. We are also thankful for the language editing services of Elsevier for editing a draft of this manuscript. This work was supported by HUSM (Hamamatsu University School of Medicine) Grant-in-Aid. This study was supported by Japan Society for the Promotion of Science (JSPS) KAKENHI Grant Numbers JP20K09325 (K.K.), JP19K09523 (T.S.).

AUTHOR CONTRIBUTIONS

T.O., H.N., and K.K. planned the conception and design. T.O., M.I., S.K., S.Y., T.Y., T. Suzuki, H.N., and K.K. developed the methodology of the experiments. T.O., M.I., M.H., and T.Y. conducted the experiments and wrote the paper. T.O., M.I., M.H., T.Y., S.K., T. Suzuki, H.N., and K.K. analyzed and interpreted the experimental data

(e.g., statistical analysis, computational analysis). M.I., T. Yamasaki, T. Suzuki, and K.K. reviewed and/or revised the manuscript. M.I., S.Y., T. Sameshima, H.S., T. Suzuki, H.N., and K.K. M.I., S.Y., T. Yamasaki, T. Sameshima, H.S., T. Suzuki, H.N., and K.K. provided administrative, technical, and material support. T. Suzuki and K.K. supervised the study.

DECLARATION OF INTERESTS

The authors declare no competing interests.

REFERENCES

1. Ferlay, J., Colombet, M., Soerjomataram, I., Mathers, C., Parkin, D.M., Piñeros, M., Znaor, A., and Bray, F. (2019). Estimating the global cancer incidence and mortality in 2018: GLOBOCAN sources and methods. Int. J. Cancer. *144*, 1941–1953. https://doi.org/10.1002/ijc.31937.

2. Sperduto, P.W., Kased, N., Roberge, D., Xu, Z., Shanley, R., Luo, X., Sneed, P.K., Chao, S.T., Weil, R.J., Suh, J., et al. (2012). Summary report on the graded prognostic assessment: an accurate and facile diagnosis-specific tool to estimate survival for patients with brain metastases. J. Clin. Oncol. *30*, 419–425. https://doi.org/10.1200/JCO.2011.38.0527.

3. Fessart, E., Mouttet Audouard, R., Le Tinier, F., Coche-Dequeant, B., Lacornerie, T., Tresch, E., Scherpereel, A., Lartigau, E., Mirabel, X., and Pasquier, D. (2020). Stereotactic irradiation of non-small cell lung cancer brain metastases: evaluation of local and cerebral control in a large series. Sci. Rep. *10*, 11201. https://doi.org/10.1038/s41598-020-68209-6.

4. Lee, S.W., Kim, Y.S., Sung, S.Y., Kwak, Y.K., Kang, Y.N., Jang, J.S., Kang, J.H., Hong, S.H., Kim, S.J., and Jung, S.L. (2020). Upfront radiosurgery plus targeted agents followed by active brain control using radiosurgery delays neurological death in non-small cell lung cancer with brain metastasis. Clin. Exp. Metastasis *37*, 353–363. https://doi.org/10.1007/s10585-020-10022-6.

5. Owonikoko, T.K., Arbiser, J., Zelnak, A., Shu, H.K.G., Shim, H., Robin, A.M., Kalkanis, S.N., Whitsett, T.G., Salhia, B., Tran, N.L., et al. (2014). Current approaches to the treatment of metastatic brain tumours. Nat. Rev. Clin. Oncol. *11*, 203–222. https://doi.org/10.1038/nrclinonc.2014.25.

6. Culver, K.W., Ram, Z., Wallbridge, S., Ishii, H., Oldfield, E.H., and Blaese, R.M. (1992). In vivo gene transfer with retroviral vector-producer cells for treatment of experimental brain tumors. Science *256*, 1550–1552. https://doi.org/10.1126/science.1317968.

7. Ram, Z., Culver, K.W., Oshiro, E.M., Viola, J.J., DeVroom, H.L., Otto, E., Long, Z., Chiang, Y., McGarrity, G.J., Muul, L.M., et al. (1997). Therapy of malignant brain tumors by intratumoral implantation of retroviral vector-producing cells. Nat. Med. *3*, 1354–1361. https://doi.org/10.1038/nm1297-1354.

8. Li, S., Gu, C., Gao, Y., Amano, S., Koizumi, S., Tokuyama, T., and Namba, H. (2012). Bystander effect in glioma suicide gene therapy using bone marrow stromal cells. Stem Cell Res. *9*, 270–276. https://doi.org/10.1016/j.scr.2012.08.002.

9. Yamasaki, T., Wakao, S., Kawaji, H., Koizumi, S., Sameshima, T., Dezawa, M., and Namba, H. (2017). Genetically engineered multilineage-differentiating stress-enduring cells as cellular vehicles against malignant gliomas. Mol. Ther. Oncolytics *6*, 45–56. https://doi.org/10.1016/j.omto.2017.06.001.

10. Amano, S., Gu, C., Koizumi, S., Tokuyama, T., and Namba, H. (2011). Tumoricidal bystander effect in the suicide gene therapy using mesenchymal stem cells does not injure normal brain tissues. Cancer Lett. *306*, 99–105. https://doi.org/10.1016/j.canlet.2011.02.037.

11. Amano, S., Li, S., Gu, C., Gao, Y., Koizumi, S., Yamamoto, S., Terakawa, S., and Namba, H. (2009). Use of genetically engineered bone marrow-derived mesenchymal stem cells for glioma gene therapy. Int. J. Oncol. *35*, 1265–1270. https://doi.org/10.3892/ijo_00000443.

12. Ibarretxe, G., Crende, O., Aurrekoetxea, M., García-Murga, V., Etxaniz, J., and Unda, F. (2012). Neural crest stem cells from dental tissues: a new hope for dental and neural regeneration. Stem Cell. Int. *2012*, 103503. https://doi.org/10.1155/2012/103503.

13. Luke, A.M., Patnaik, R., Kuriadom, S., Abu-Fanas, S., Mathew, S., and Shetty, K.P. (2020). Human dental pulp stem cells differentiation to neural cells, osteocytes and adipocytes-An in vitro study. Heliyon *6*, e03054. https://doi.org/10.1016/j.heliyon.2019.e03054.

14. Huang, G.T.J., Gronthos, S., and Shi, S. (2009). Mesenchymal stem cells derived from dental tissues vs. those from other sources: their biology and role in regenerative medicine. J. Dent. Res. *88*, 792–806. https://doi.org/10.1177/0022034509340867.

15. Ishizaka, R., Hayashi, Y., Iohara, K., Sugiyama, M., Murakami, M., Yamamoto, T., Fukuta, O., and Nakashima, M. (2013). Stimulation of angiogenesis, neurogenesis and regeneration by side population cells from dental pulp. Biomaterials *34*, 1888–1897. https://doi.org/10.1016/j.biomaterials.2012.10.045.

16. Zhang, X., Zhou, Y., Li, H., Wang, R., Yang, D., Li, B., Cao, X., and Fu, J. (2018). Transplanted dental pulp stem cells migrate to injured area and express neural markers in a rat model of cerebral ischemia. Cell. Physiol. Biochem. *45*, 258–266. https://doi.org/10.1159/000486772.

17. Iwasawa, C., Tamura, R., Sugiura, Y., Suzuki, S., Kuzumaki, N., Narita, M., Suematsu, M., Nakamura, M., Yoshida, K., Toda, M., et al. (2019). Increased cytotoxicity of herpes simplex virus thymidine kinase expression in human induced pluripotent stem cells. Int. J. Mol. Sci. *20*, E810. https://doi.org/10.3390/ijms20040810.

18. Balzarini, J., Liekens, S., Solaroli, N., El Omari, K., Stammers, D.K., and Karlsson, A. (2006). Engineering of a single conserved amino acid residue of herpes simplex virus type 1 thymidine kinase allows a predominant shift from pyrimidine to purine nucleoside phosphorylation. J. Biol. Chem. *281*, 19273–19279. https://doi.org/10.1074/jbc.M600414200.

19. Ryu, C.H., Park, K.Y., Kim, S.M., Jeong, C.H., Woo, J.S., Hou, Y., and Jeun, S.S. (2012). Valproic acid enhances anti-tumor effect of mesenchymal stem cell mediated HSV-TK gene therapy in intracranial glioma. Biochem. Biophys. Res. Commun. *421*, 585–590. https://doi.org/10.1016/j.bbrc.2012.04.050.

20. Tamura, R., Miyoshi, H., Morimoto, Y., Oishi, Y., Sampetrean, O., Iwasawa, C., Mine, Y., Saya, H., Yoshida, K., Okano, H., and Toda, M. (2020). Gene therapy using neural stem/progenitor cells derived from human induced pluripotent stem cells: visualization of migration and bystander killing effect. Hum. Gene. Ther. *31*, 352–366. https://doi.org/10.1089/hum.2019.326.

21. Preuss, E., Treschow, A., Newrzela, S., Brücher, D., Weber, K., Felldin, U., Alici, E., Gahrton, G., von Laer, D., Dilber, M.S., and Fehse, B. (2010). TK.007: a novel, codon-optimized HSVtk(A168H) mutant for suicide gene therapy. Hum. Gene. Ther. *21*, 929–941. https://doi.org/10.1089/hum.2009.042.

22. Preuss, E., Muik, A., Weber, K., Otte, J., von Laer, D., and Fehse, B. (2011). Cancer suicide gene therapy with TK.007: superior killing efficiency and bystander effect. J. Mol. Med. *89*, 1113–1124. https://doi.org/10.1007/s00109-011-0777-8.

23. Black, M.E., Kokoris, M.S., and Sabo, P. (2001). Herpes simplex virus-1 thymidine kinase mutants created by semi-random sequence mutagenesis improve prodrug-mediated tumor cell killing. Cancer Res. *61*, 3022–3026.

24. Nouri, F.S., Wang, X., and Hatefi, A. (2015). Genetically engineered theranostic mesenchymal stem cells for the evaluation of the anticancer efficacy of enzyme/prodrug systems. J. Control. Release *200*, 179–187. https://doi.org/10.1016/j.jconrel.2015.01.003.

25. Bonnekoh, B., Greenhalgh, D.A., Bundman, D.S., Eckhardt, J.N., Longley, M.A., Chen, S.H., Woo, S.L., and Roop, D.R. (1995). Inhibition of melanoma growth by adenoviral-mediated HSV thymidine kinase gene transfer in vivo. J. Invest. Dermatol. *104*, 313–317. https://doi.org/10.1111/1523-1747.ep12664614.

26. Määttä, A.M., Tenhunen, A., Pasanen, T., Meriläinen, O., Pellinen, R., Mäkinen, K., Alhava, E., and Wahlfors, J. (2004). Non-small cell lung cancer as a target disease for herpes simplex type 1 thymidine kinase-ganciclovir gene therapy. Int. J. Oncol. *24*, 943–949.

27. Wang, J., Lu, X.X., Chen, D.Z., Li, S.F., and Zhang, L.S. (2004). Herpes simplex virus thymidine kinase and ganciclovir suicide gene therapy for human pancreatic cancer. World. J. Gastroenterol. *10*, 400–403. https://doi.org/10.3748/wjg.v10.i3.400.

28. Kuo, W.Y., Hwu, L., Wu, C.Y., Lee, J.S., Chang, C.W., and Liu, R.S. (2017). STAT3/NF-kappaB-Regulated lentiviral TK/GCV suicide gene therapy for cisplatin-resistant triple-negative breast cancer. Theranostics *7*, 647–663. https://doi.org/10.7150/thno.16827.

29. Joo, K.M., Park, I.H., Shin, J.Y., Jin, J., Kang, B.G., Kim, M.H., Lee, S.J., Jo, M.Y., Kim, S.U., and Nam, D.H. (2009). Human neural stem cells can target and deliver therapeutic genes to breast cancer brain metastases. Mol. Ther. *17*, 570–575. https://doi.org/10.1038/mt.2008.290.

30. Wang, C., Natsume, A., Lee, H.J., Motomura, K., Nishimira, Y., Ohno, M., Ito, M., Kinjo, S., Momota, H., Iwami, K., et al. (2012). Neural stem cell-based dual suicide gene delivery for metastatic brain tumors. Cancer Gene. Ther. *19*, 796–801. https://doi.org/10.1038/cgt.2012.63.

31. Yi, B.R., Kim, S.U., Kim, Y.B., Lee, H.J., Cho, M.H., and Choi, K.C. (2012). Antitumor effects of genetically engineered stem cells expressing yeast cytosine deaminase in lung cancer brain metastases via their tumor-tropic properties. Oncol. Rep. *27*, 1823–1828. https://doi.org/10.3892/or.2012.1721.

32. Corban-Wilhelm, H., Becker, G., Bauder-Wüst, U., Greulich, D., and Debus, J. (2003). Cytosine deaminase versus thymidine kinase: a comparison of the antitumor activity. Clin. Exp. Med. *3*, 150–156. https://doi.org/10.1007/s10238-003-0018-8.

33. Sangro, B., Mazzolini, G., Ruiz, M., Ruiz, J., Quiroga, J., Herrero, I., Qian, C., Benito, A., Larrache, J., Olagüe, C., et al. (2010). A phase I clinical trial of thymidine kinase-based gene therapy in advanced hepatocellular carcinoma. Cancer Gene. Ther. *17*, 837–843. https://doi.org/10.1038/cgt.2010.40.

34. Kim, K.H., Dmitriev, I., O'Malley, J.P., Wang, M., Saddekni, S., You, Z., Preuss, M.A., Harris, R.D., Aurigemma, R., Siegal, G.P., et al. (2012). A phase I clinical trial of Ad5.SSTR/TK.RGD, a novel infectivity-enhanced bicistronic adenovirus, in patients with recurrent gynecologic cancer. Clin. Cancer Res. *18*, 3440–3451. https://doi.org/10.1158/1078-0432.CCR-11-2852.

35. Freytag, S.O., Stricker, H., Lu, M., Elshaikh, M., Aref, I., Pradhan, D., Levin, K., Kim, J.H., Peabody, J., Siddiqui, F., et al. (2014). Prospective randomized phase 2 trial of intensity modulated radiation therapy with or without oncolytic adenovirus-mediated cytotoxic gene therapy in intermediate-risk prostate cancer. Int. J. Radiat. Oncol. Biol. Phys. *89*, 268–276. https://doi.org/10.1016/j.ijrobp.2014.02.034.

36. Lee, J.C., Shin, D.W., Park, H., Kim, J., Youn, Y., Kim, J.H., Kim, J., and Hwang, J.H. (2020). Tolerability and safety of EUS-injected adenovirus-mediated double-suicide gene therapy with chemotherapy in locally advanced pancreatic cancer: a phase 1 trial. Gastrointest. Endosc. *92*, 1044–1052.e1. https://doi.org/10.1016/j.gie.2020.02.012.

37. Zhao, D., Najbauer, J., Garcia, E., Metz, M.Z., Gutova, M., Glackin, C.A., Kim, S.U., and Aboody, K.S. (2008). Neural stem cell tropism to glioma: critical role of tumor hypoxia. Mol. Cancer Res. *6*, 1819–1829. https://doi.org/10.1158/1541-7786.MCR-08-0146.

38. Koizumi, S., Gu, C., Amano, S., Yamamoto, S., Ihara, H., Tokuyama, T., and Namba, H. (2011). Migration of mouse-induced pluripotent stem cells to glioma-conditioned medium is mediated by tumor-associated specific growth factors. Oncol. Lett. *2*, 283–288. https://doi.org/10.3892/ol.2011.234.

39. Nosrat, I.V., Widenfalk, J., Olson, L., and Nosrat, C.A. (2001). Dental pulp cells produce neurotrophic factors, interact with trigeminal neurons in vitro, and rescue motoneurons after spinal cord injury. Dev. Biol. *238*, 120–132. https://doi.org/10.1006/dbio.2001.0400.

40. Ahmed, N.E.M.B., Murakami, M., Kaneko, S., and Nakashima, M. (2016). The effects of hypoxia on the stemness properties of human dental pulp stem cells (DPSCs). Sci. Rep. *6*, 35476. https://doi.org/10.1038/srep35476.

41. Kenmochi, H., Yamasaki, T., Koizumi, S., Sameshima, T., and Namba, H. (2020). Nicotine does not affect stem cell properties requisite for suicide gene therapy against glioma. Neurol. Res. *42*, 818–827. https://doi.org/10.1080/01616412.2020.1782123.

42. Anoop, M., and Datta, I. (2021). Stem cells derived from human exfoliated deciduous teeth (SHED) in neuronal disorders: a review. Curr. Stem Cell Res. Ther. *16*, 535–550. https://doi.org/10.2174/1574888X16666201221151512.

43. Miura, M., Gronthos, S., Zhao, M., Lu, B., Fisher, L.W., Robey, P.G., and Shi, S. (2003). SHED: stem cells from human exfoliated deciduous teeth. Proc. Natl. Acad. Sci. USA *100*, 5807–5812. https://doi.org/10.1073/pnas.0937635100.

44. Suchánek, J., Visek, B., Soukup, T., El-Din Mohamed, S.K., Ivancaková, R., Mokrỳ, J., Aboul-Ezz, E.H.A., and Omran, A. (2010). Stem cells from human exfoliated deciduous teeth–isolation, long term cultivation and phenotypical analysis. Acta Medica. *53*, 93–99. https://doi.org/10.14712/18059694.2016.66.

45. Zhang, G., Shang, B., Yang, P., Cao, Z., Pan, Y., and Zhou, Q. (2012). Induced pluripotent stem cell consensus genes: implication for the risk of tumorigenesis and cancers in induced pluripotent stem cell therapy. Stem Cell. Dev. *21*, 955–964. https://doi.org/10.1089/scd.2011.0649.

46. Wilson, R., Urraca, N., Skobowiat, C., Hope, K.A., Miravalle, L., Chamberlin, R., Donaldson, M., Seagroves, T.N., and Reiter, L.T. (2015). Assessment of the tumorigenic potential of spontaneously immortalized and hTERT-immortalized cultured dental pulp stem cells. Stem Cell. Transl. Med. *4*, 905–912. https://doi.org/10.5966/sctm.2014-0196.

47. Shin, D.Y., Na, I.I., Kim, C.H., Park, S., Baek, H., and Yang, S.H. (2014). EGFR mutation and brain metastasis in pulmonary adenocarcinomas. J. Thorac. Oncol. *9*, 195–199. https://doi.org/10.1097/JTO.0000000000000069.

48. Vakhshiteh, F., Atyabi, F., and Ostad, S.N. (2019). Mesenchymal stem cell exosomes: a two-edged sword in cancer therapy. Int. J. Nanomed. *14*, 2847–2859. https://doi.org/10.2147/IJN.S200036.

49. Tibensky, M., Jakubechova, J., Altanerova, U., Pastorakova, A., Rychly, B., Baciak, L., Mravec, B., and Altaner, C. (2022). Gene-directed enzyme/prodrug therapy of rat brain tumor mediated by human mesenchymal stem cell suicide gene extracellular vesicles in vitro and in vivo. Cancers *14*, 735. https://doi.org/10.3390/cancers14030735.

50. Heidarzadeh, M., Gürsoy-Özdemir, Y., Kaya, M., Eslami Abriz, A., Zarebkohan, A., Rahbarghazi, R., and Sokullu, E. (2021). Exosomal delivery of therapeutic modulators through the blood-brain barrier; promise and pitfalls. Cell Biosci. *11*, 142. https://doi.org/10.1186/s13578-021-00650-0.

51. Wagner, M.J., Sharp, J.A., and Summers, W.C. (1981). Nucleotide sequence of the thymidine kinase gene of herpes simplex virus type 1. Proc. Natl. Acad. Sci. USA *78*, 1441–1445. https://doi.org/10.1073/pnas.78.3.1441.